

Separating Binary Gaseous Mixtures of Ethene + Ethyne Using Cement Hydrate: A Multiscale Computational Study

Matthew Lasich*

Cite This: *ACS Omega* 2021, 6, 19940–19945

Read Online

ACCESS |



Metrics & More

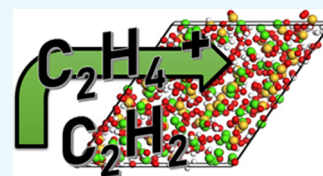


Article Recommendations



Supporting Information

ABSTRACT: Cement production is a carbon intensive industry and is responsible for large quantities of greenhouse gases released into the atmosphere. Due to the significant embedded carbon costs of cement, it might be promising to investigate waste cement for alternative uses so as to maximize utility of this material. Recent computational work on the sorption of natural gas constitutions in cement hydrate suggested that it might be worthwhile examining its usefulness in separating mixtures of C_2 hydrocarbons. In light of this and the ongoing challenges of separating ethene and ethyne in industry, this study employed a multiscale approach to assess the feasibility of pressure swing adsorption to separate mixtures of ethene + ethyne. By combining stochastic atomistic simulations with macroscale batch equilibrium modeling, ethene recovery, product gas composition, and the separation power were computed over a range of temperatures (from 273 to 323 K), pressures (100 to 2000 kPa), and adsorbent masses (10 to 40 g per mole of feed gas). The results of this study include a look at the intermolecular interactions in the system and their relationship to the adsorption behavior as described by well-known adsorption isotherm models. This can help point the way to selecting materials that are promising for gas separations.



1. INTRODUCTION

Concrete is a composite material consisting of an aggregate phase and a binding phase, with a cement hydrate matrix comprising the binding phase. Tricalcium silicate, dicalcium silicate, and tricalcium aluminate are major components of the binding phase, and they react with water to form three main hydration products: calcium-silicate hydrate, ettringite, and portlandite.¹ Production of cement is an environmental concern both due to significant carbon emissions² and water consumption.³ Concrete infrastructure and buildings, containing large quantities of cement hydrate, therefore constitute a significant amount of embedded carbon worldwide. Hence, it can be advantageous if more uses can be found for waste cement, to enable the introduction of additional recycling streams for this material thereby maximizing the utility of its embedded carbon.

Recent work on the molecular interactions of natural gas constituents with cement hydrate (with a focus on hydrogen sulfide)⁴ yielded results that (incidentally) suggested that cement hydrate might have potential use in separating mixtures of ethane/ethene/ethyne. Since all three species have purely dispersive interactions with the cement hydrate matrix, this is largely due to reduced molecular sizes. Ethyne is a more compact molecule than ethene due to both the reduced number of hydrogen atoms (rendering ethyne more rodlike than ethene, which has a dumbbell-like shape in comparison) and the shorter length of the triple carbon bond as compared to the double carbon bond. The reduced molecular volume of ethyne as compared to ethene therefore enables more ethyne molecules to fit into the tortuous cavities within the cement hydrate matrix. Ethene (C_2H_4 , commonly called ethylene) is one of the most widely used basic petrochemicals and is employed as a precursor

for larger organic compounds and to produce polyethylene via polymerization. In the production of polyethylene, very high purity ethene is required and necessitates the separation of ethene from ethyne (C_2H_2 , commonly called acetylene), which typically occur together following the cracking of naphtha or ethane/propane mixtures. The presence of ethyne in the ethene feedstock for polyethylene production in quantities as low as 40 ppm can poison the Ziegler-Natta catalysts needed for this process,⁵ and excess ethyne can block gas flow with potentially explosive results via the generation of solid acetylides.⁶ The necessary ethene is generally prepared by the cryogenic distillation of cracking gas, which typically results in an unavoidable impurity of 1 mol % ethyne that requires further separation before downstream processing of the ethene to produce other materials.⁷

Presently, adsorption offers an attractive energy-efficient option for this purification step as compared to conventional methods such as partial hydrogenation or solvent extraction.^{8–10} Much recent work has examined the use of microporous or nanoporous materials such as metal–organic frameworks^{7,8,10–13} as adsorbents for the separation of ethene and ethyne.

Received: June 3, 2021

Accepted: July 13, 2021

Published: July 21, 2021



This contribution is concerned with evaluating the potential efficacy of cement hydrate as an adsorbent for the separation of ethene/ethyne mixtures via pressure swing adsorption cycles near ambient temperature. In particular, several variables were considered for the pressure swing adsorption process: operating pressure ratio, ratio of the adsorbent mass to feed gas flow rate (i.e., the bed size), operating temperature, and feed gas composition. The resulting outputs to be considered were the ethylene recovery, product gas composition in terms of ethene purity, and the ethene/ethyne separation power. Monte Carlo molecular simulations¹⁴ in the grand canonical ensemble were used to generate adsorption isotherm data necessary for evaluating the pressure swing adsorption cycles, which was undertaken using a macroscale batch equilibrium approach.¹⁵

2. RESULTS AND DISCUSSION

Figures 1 and 2 show the adsorption isotherms for ethene and ethyne, respectively, at 273, 298, and 323 K. Apart from the

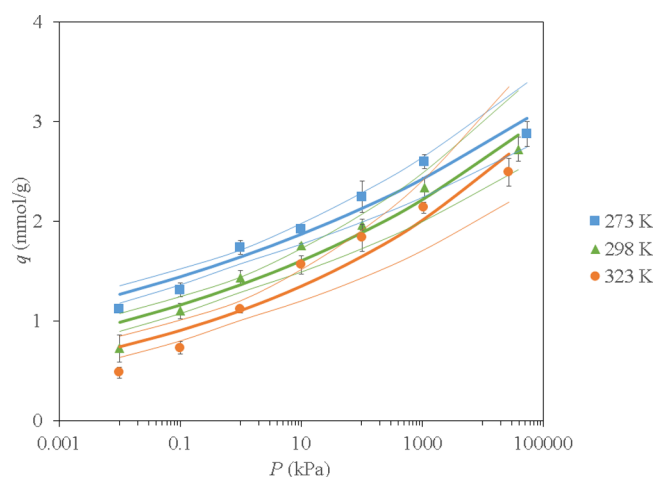


Figure 1. Adsorption isotherms for ethene in cement hydrate. The curves shown are for the fitted Freundlich adsorption isotherm model. Note that the x -axis has been made logarithmic for clarity. The thin lines represent the 95% confidence intervals for each fitted isotherm.

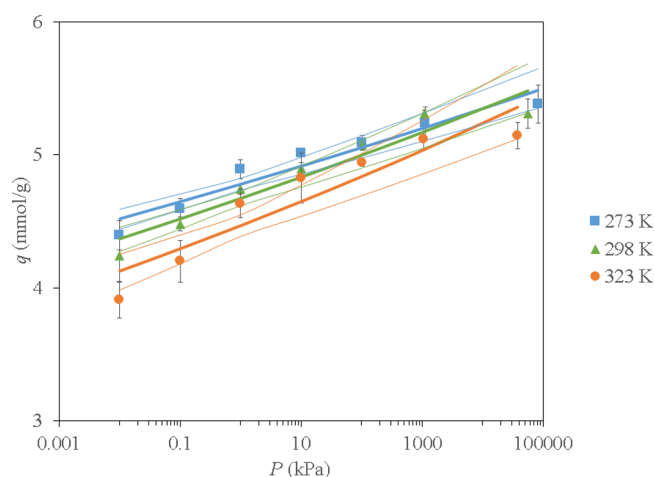


Figure 2. Adsorption isotherms for ethyne in cement hydrate. The curves shown are for the fitted Freundlich adsorption isotherm model. Note that the x -axis has been made logarithmic for clarity. The thin lines represent the 95% confidence intervals for each fitted isotherm.

results of the Monte Carlo simulations, fitted adsorption isotherm models are shown. These are needed for the batch equilibrium modeling, hence it was necessary to determine which adsorption isotherm model provides the most accurate description of the results of the simulations. To that end, three models were considered: Langmuir,¹⁶ Freundlich,¹⁷ and Redlich–Peterson.¹⁸ In both Figures 1 and 2, the Freundlich adsorption isotherm model is shown alongside the results of the molecular simulations, as it produced the best fit.

The Langmuir and Freundlich models are both two parameter models, with the former being possibly the simplest means of describing adsorption of fluid molecules onto a substrate. The Langmuir adsorption isotherm model is based upon the following assumptions: monolayer adsorption, finite localized adsorption sites that are identical and equivalent, and no lateral interaction or steric hindrance between adsorbed molecules. The Freundlich model accounts for nonideal and reversible adsorption, as well as a nonuniform distribution of adsorption heats and affinities across a heterogeneous surface. The three-parameter Redlich–Peterson model is a hybrid isotherm that incorporates features of both the Langmuir and Freundlich models and approaches the Langmuir model at low pressures/concentrations while approaching the Freundlich model at high pressures/concentrations. The three adsorption isotherm models are presented below:

$$q = \frac{QbP}{1 + bP} \quad (1)$$

$$q = KP^{1/n} \quad (2)$$

$$q = \frac{kP}{1 + aP^h} \quad (3)$$

wherein q is the quantity of gas adsorbed, P is the gas pressure, and Q , b , K , n , k , a , and h are parameters fitted to the results of the simulations. In the Langmuir model, Q represents the saturation sorption capacity, while b is the Langmuir equilibrium constant. In the Freundlich model, K is the Freundlich constant indicating adsorption capacity and $1/n$ describes the heterogeneity of the surface. Lastly, in the Redlich–Peterson model, k/a indicates the adsorption capacity and h is a constant whereby if it is equal to 1, the Langmuir equation is returned. The results of the parameter fitting are shown in Tables 1–3, for each adsorption model in turn. The correlation coefficient (R^2) and the percentage absolute average deviation (%AAD) are presented to demonstrate the quality of the fitted models.

It can be noted that while the R^2 values for the Freundlich and Redlich–Peterson models are comparable, the %AAD values for

Table 1. Fitted Parameters, R^2 , and %AAD for the Langmuir Isotherm Model^a

T (K)	b (kPa ⁻¹)	Q (mmol.g ⁻¹)	R^2	%AAD
ethene				
273	51.06 ± 47.00	2.220 ± 0.224	0.7113	21.95
298	11.95 ± 10.26	2.095 ± 0.218	0.8269	23.69
323	1.758 ± 1.401	2.032 ± 0.210	0.9184	32.00
ethyne				
273	604.5 ± 263.9	5.060 ± 0.105	0.7563	3.384
298	510.2 ± 240.7	4.996 ± 0.126	0.7375	4.497
323	374.6 ± 154.7	4.846 ± 0.131	0.7940	4.606

^a95% confidence intervals are given for the fitted parameters.

Table 2. Fitted Parameters, R^2 , and %AAD for the Freundlich Isotherm Model^a

T (K)	K (mmol.g ⁻¹ .kPa ^{-1/n})	n	R^2	%AAD
ethene				
273	1.644 ± 0.069	17.77 ± 1.82	0.9769	6.900
298	1.365 ± 0.076	14.23 ± 1.54	0.9762	9.908
323	1.106 ± 0.098	11.55 ± 1.58	0.9663	16.50
ethyne				
273	4.780 ± 0.045	82.16 ± 10.32	0.9629	1.636
298	4.673 ± 0.055	68.39 ± 9.10	0.9604	2.324
323	4.468 ± 0.081	57.92 ± 10.24	0.9315	3.239

^a95% confidence intervals are given for the fitted parameters.**Table 3. Fitted Parameters, R^2 , and %AAD for the Redlich–Peterson Isotherm Model^a**

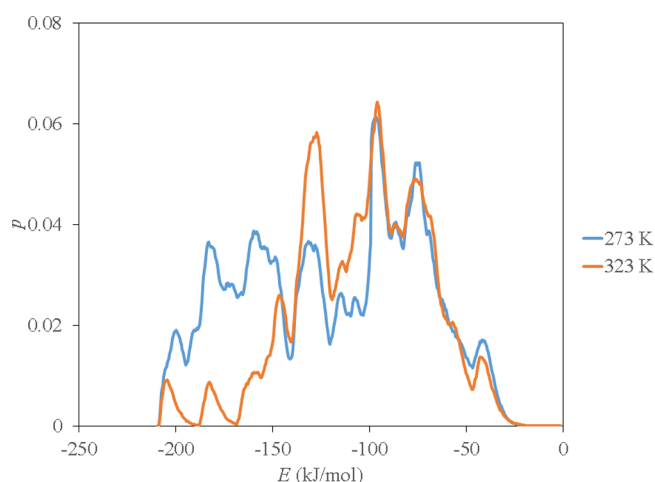
T (K)	k (mmol.g ⁻¹ .kPa ^{-h})	a (kPa ^{-h})	h	R^2	%AAD
ethene					
273	549.6 ± 388.5	320.6 ± 233.9	0.9490 ± 0.0061	0.9855	4.408
298	182.0 ± 62.0	123.1 ± 43.8	0.9399 ± 0.0047	0.9949	3.813
323	63.17 ± 40.81	50.81 ± 34.49	0.9281 ± 0.0102	0.9861	1.089
ethyne					
273	8342 ± 3546	1721 ± 741	0.9899 ± 0.0014	0.9848	0.9435
298	7585 ± 4608	1600 ± 985	0.9875 ± 0.0021	0.9760	1.273
323	3898 ± 1817	850.1 ± 405.5	0.9867 ± 0.0029	0.9696	1.985

^a95% confidence intervals are given for the fitted parameters.

the Redlich–Peterson model are better, in relative terms, than those for the Freundlich model. While the Redlich–Peterson model produced a slightly closer fit to the results of the simulations than the Freundlich model, the 95% confidence intervals for the fitted parameters are rather large, which would make subsequent secondary analysis unreliable. Hence, the Freundlich model was used for batch equilibrium modeling of a single-stage pressure swing adsorption system. While the %AAD for the Freundlich model is significantly larger than that for the Redlich–Peterson model in some situations (notably for ethene at 323 K), it should be noted that this was due to substantial deviations at very low pressure values, which is outside the range of interest for the purposes of analyzing the performance of pressure swing adsorption in this study.

In terms of the influence of parameter variance on the results of secondary analyses, it can be instructive to consider the predicted adsorption isotherms for ethene and ethyne relative to one another, as shown in Figures 1 and 2. Comparing the bounds of the 95% confidence intervals for the fitted curves, it is apparent that there is no risk of drastic variation in the ratios of the adsorbed quantities of gas, which is the variable of interest in pressure swing adsorption modeling using the batch equilibrium approach. Moreover, in all cases (except for ethene at very low pressure at 323 K, which is below the pressure range of interest in the study in any case), the 95% confidence interval for the fitted Freundlich adsorption isotherms lie within one standard deviation of the results of the grand canonical Monte Carlo simulations, indicating the robustness of the Freundlich isotherm with regard to describing the system at hand.

In terms of the behavior of the adsorption isotherms, it is clear that neither species is adequately described by the Langmuir approach, although at higher temperatures the correlation coefficient tends to increase. With respect to the Freundlich model, it generally described the behavior of the system better at lower temperatures. These outcomes can be better understood by examining the energies of the systems at 273 and 323 K, as shown in Figure 3. Since the difference in the quality of the fit for

**Figure 3.** Distribution of interaction energies E for ethyne in cement hydrate at 273 compared to 323 K at the maximum pressure value considered in this study, where p is the likelihood of occurrence. Values are averaged across three independent simulations.

the Langmuir versus Freundlich models was larger for ethyne than that for ethene, it is instructive to consider it instead of ethene. It is apparent that at higher temperatures the bandwidth between the upper and lower bounds of the standard deviation is larger at 273 K as compared to 323 K, suggesting an increase in the degree of uniformity in terms of the magnitude of the intermolecular interactions, which likely explains the observations for the Langmuir model fitting better at higher temperatures and the Freundlich model working better at lower temperatures, since a narrower bandwidth for the interaction energies suggests a greater degree of uniformity in the intermolecular interactions, a key difference between the Langmuir and Freundlich models. With respect to selecting adsorbents for this challenging gas separation task, these results suggest that the distribution of intermolecular energies can provide some predictive insights in terms of the adsorption behavior. Selecting an adsorption with significantly stronger species-specific interactions that have only a narrow range of probable interaction energy values would be most desirable and would also permit the use of the simplistic Langmuir model to describe the system accurately.

The temperature, bed size (in grams per mole of feed gas), feed gas composition (as described in terms of the ethene mole fraction for the binary ethene/ethyne feed), and the operating pressure ratio (i.e., the ratio of the peak adsorption pressure to the discharge pressure) were simultaneously varied to generate response surfaces for the PSA system in terms of ethene recovery, composition of ethene in the product gas, and ethene/ethyne separation power. The separation power SP is expressed as follows:

$$SP = \left(\frac{p_{C_2H_4}}{f_{C_2H_4}} \right) \left(\frac{p_{C_2H_2}}{f_{C_2H_2}} \right) \quad (4)$$

where p_i is the quantity of a particular component in the product gas (discharged from the PSA system) and f_i is the quantity of the same species in the feed gas. In all cases the feed and discharge pressure were 101.3 kPa, and therefore, the operating pressure ratio is determined by dividing the peak adsorption pressure by 101.3 kPa. Table 4 summarizes the variation in the

Table 4. Summary of the Manipulated Variables Used to Investigate the Performance of a Single-Stage PSA System to Separate an Ethene/Ethyne Mixture under Isothermal Conditions

variable	minimum value	maximum value
temperature	273 K	323 K
bed mass	10 g/mol	40 g/mol
operating pressure ratio	10	200
ethene content in the feed	25 mol %	75 mol %

manipulated variables. In all cases, the manipulated variables were varied in three linearly spaced steps simultaneously, thus generating results for four values of each.

For feed gas containing 75 mol % ethene, the peak separation power was obtained at a bed mass of 40 g/mol and an operating pressure ratio of 200, whereas for the other feed gas compositions (25 and 50 mol % ethene), the optimal operating pressure ratio was 10 (the reader is referred to the Supporting Information data for the full set of response surface results). To quantify observations further, the peak separation power was assessed in terms of the feed composition and the operating temperature. These results are plotted as a response surface as shown in Figure 4, which indicates that the most effective

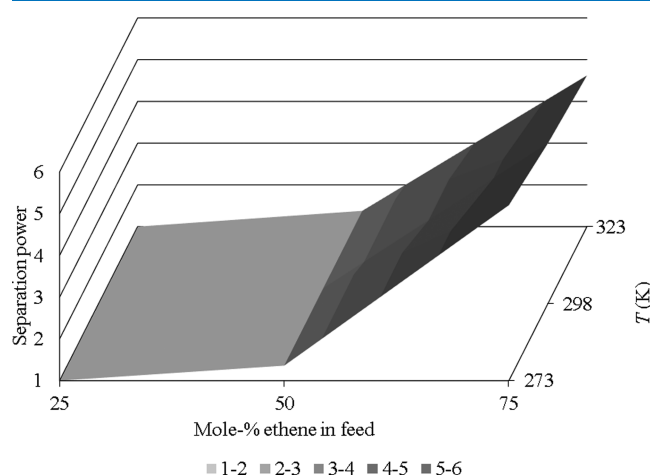


Figure 4. Response surface for the peak separation power for separating ethene from a binary ethene/ethyne mixture using a single-stage PSA system in terms of the feed composition and operating temperature.

separation occurs at high levels of ethene content in the feed gas. This suggests that cement hydrate, if it is to be used, should be used for purification rather than bulk separation at low concentrations of ethene in ethene/ethyne gas mixtures for which it is actually incapable of improving the concentration of ethyne in the product gas when the feed gas contains ethene concentrations as low as 25 mol %. In addition, lower

temperatures are preferred to boost the efficacy of separation under these conditions. However, the separation power is still rather low, even in the best-case scenario, with a maximum value of 5.21 for the range of conditions considered in this study. It may be noted that due to the limited efficacy of the system at close to ambient conditions, it was deemed to not be worthwhile extending the investigation to significantly higher or lower temperatures; such conditions would likely only increase operating costs in practical terms while not providing sufficient enhancement. More suitable adsorbents in terms of selectivity would be metal–organic frameworks such as UTSA-100a,¹⁹ M'MOF-3a,¹⁹ SIFSIX-2-Cu-i,¹² ELM-12,¹² or UTSA-300,¹³ or possibly mesoporous silica SBA-15.²⁰ Commercial zeolite 13X also exhibits superior characteristics as an adsorbent;²¹ hence, it is not recommended that cement hydrate and thus waste cement or concrete should be used as an adsorbent for separating binary mixtures of ethene and ethyne.

3. CONCLUSIONS

Monte Carlo molecular simulations in the grand canonical ensemble were used to generate adsorption isotherms for ethene and ethyne in cement hydrate. In all cases, the Redlich–Peterson adsorption isotherm model best described the adsorption behavior, on account of the distribution in magnitude of the intermolecular interactions for both species. This fitted adsorption isotherm was then coupled with a batch equilibrium approach to model a single-stage PSA system operating under isothermal conditions.

The computer model of the PSA was tested over a range of bed masses, operating pressure ratios, feed compositions, and temperatures to assess the separation power, ethene recovery, and product gas composition. It was observed that the system functions best at higher temperatures and higher operating pressure ratios. The best separation powers were achieved at low temperature (273 K) and high ethene content in the feed (75 mol %), suggesting that cement hydrate is most appropriate under these conditions. However, the peak separation power was only about 5.21, thus indicating that other adsorbents such as metal–organic frameworks or commercial zeolites are probably preferable to cement hydrate for separating mixtures of ethene and ethyne.

4. COMPUTATIONAL METHODS

An atomistic molecular model of calcium-silicate-hydrate from the literature²² that accurately predicts essential features and fundamental physical properties of the material was used. This structure has been used previously, with some success, to describe sorption of natural gas with cement hydrate.⁴ In summary, the cement hydrate structure comprises a network of short silica chains distributed as monomers, dimers, and pentamers in a gel-like matrix with both crystalline and glassy features of the mineral tobermorite. The unit cell for this structure is $H_{196}O_{317}Si_{160}Ca_{99}$.

Adsorption in the solid cement hydrate phase was described using Monte Carlo simulations following the Metropolis scheme¹⁴ in the grand canonical ensemble for which the volume of the simulation cell, fluid reservoir chemical potential, and temperature are held constant. Version 2020 of Materials Studio was used for all of the Monte Carlo simulations.²³ This ensemble mimics migration into and out of the adsorbent by permitting the following moves applied to the gas molecules (with probabilities of occurrence in parentheses): creation (0.23),

deletion (0.23), rotation (0.24), translation (0.24), and regrowth (0.06). The general methodology of the simulations employed in this work is similar to previous work,²⁴ although in this study 2×10^7 Monte Carlo moves were used for equilibration followed a further 2×10^7 moves to generate results, and the results were averaged across three independent simulations. This increased simulation time ensured that there was no doubt that equilibration was achieved, especially at higher gas fugacities where there were more adsorbed molecules in the cement hydrate phase. Fugacities were related to pressures using the ubiquitous Peng–Robinson cubic equation of state.²⁵

Version 3 of the condensed-phase-optimized molecular potentials for atomistic simulation studies (COMPASS) was used in this work.²⁶ The COMPASS force field was successfully utilized recently for the natural gas + cement hydrate system⁴ for which it was found that system size effects were negligible in terms of artificial periodicity artifacts, and so in this study, a single unit cell was used with a cutoff radius of 1.85 nm for van der Waals interactions and Ewald summation for long-range electrostatic forces.²⁷ Details of the COMPASS force field and its applicability to the present system can be found in the literature.⁴

Batch equilibrium modeling was undertaken according to the method described in a recently published study,²⁴ which was based on a shortcut method for evaluating the efficacy of PSA systems.¹⁵ This approach was implemented in version 5.1.0 of GNU Octave²⁸ to generate the response surface information for single-stage pressure swing adsorption separation of ethene from ethene + ethyne mixtures.

To describe adsorption of the gas mixture, in principle either competitive or noncompetitive adsorption could be considered. In the former approach, fitting to mixture data would be required when employing the Freundlich isotherm, whereas mixture adsorption can be estimated without mixture data when using the Langmuir or Redlich–Peterson isotherms. With non-competitive adsorption, the different gas species in the mixture are considered to adsorb at different locations, and thus, the adsorption of each species can be described separately without the need for mixture properties. In this study, the image processing package implemented in GNU Octave was employed to determine the correlation coefficient between field densities of the adsorbed ethene and ethyne molecules at the maximum uptake for both species (which occurred at 273 K and the maximum pressure values for each species). A simulation comprising 2×10^7 Monte Carlo moves for each equilibration and production, with sampling every 25 moves during production was used to build up a three-dimensional map of adsorption sites for each species. This was used to generate a field map from which two different views were converted into PNG images (1070×571 pixels), which were colored by distance from the observer (higher color saturation corresponding to a shorter distance from the viewpoint). In these field maps, the atoms comprising the cement hydrate matrix were removed, thereby producing images consisting solely of the adsorption sites. The correlation coefficients for each perspective were approximately 0.099 and 0.282, thus suggesting that there is little similarity in the locations of adsorption sites for ethene and ethyne, and hence noncompetitive adsorption was deduced to occur at the conditions of interest. These field maps are provided in the [Supporting Information](#).

■ ASSOCIATED CONTENT

■ Supporting Information

The Supporting Information is available free of charge at <https://pubs.acs.org/doi/10.1021/acsomega.1c02902>.

Response surface results for batch equilibrium modeling of a single-stage pressure swing adsorption system, along with field maps of the adsorption sites for ethene and ethyne in cement hydrate (PDF)

■ AUTHOR INFORMATION

Corresponding Author

Matthew Lasich – Department of Chemical Engineering, Mangosuthu University of Technology, Durban 4031, South Africa; orcid.org/0000-0002-7849-6603; Email: lasich.matthew@mut.ac.za

Complete contact information is available at: <https://pubs.acs.org/doi/10.1021/acsomega.1c02902>

Notes

The author declares no competing financial interest.

■ ACKNOWLEDGMENTS

All simulations were performed using the facilities of the Centre for High Performance Computing (CHPC) in Cape Town, South Africa. This work is supported by the National Research Foundation (NRF) through its Rated Researcher program.

■ REFERENCES

- (1) Lau, D.; Jian, W.; Yu, Z.; Hui, D. Nano-engineering of construction materials using molecular dynamics simulations: prospects and challenges. *Compos. B Eng.* **2018**, *143*, 282–291.
- (2) Mahasenan, N.; Smith, S.; Humphreys, K.; Kaya, Y. The cement industry and global climate change: current and potential future cement industry CO₂ emissions. In *Greenhouse Gas Control Technologies – 6th International Conference, Kyoto, Japan, October 1–4, 2002*; Gale, J.; Kaya, Y. Eds.; Pergamon: Oxford, 2003; 995–1000.
- (3) Miller, S. A.; Horvath, A.; Monteiro, P. J. M. Impacts of booming concrete production on water resources worldwide. *Nat. Sustain.* **2018**, *1*, 69–76.
- (4) Lasich, M. Sorption of natural gas in cement hydrate by Monte Carlo simulation. *Eur. Phys. J. B* **2018**, *91*, 299.
- (5) Huang, W.; McCormick, J. R.; Lobo, R. F.; Chen, J. G. Selective hydrogenation of acetylene in the presence of ethylene on zeolite-supported bimetallic catalysts. *J. Catal.* **2007**, *246*, 40–51.
- (6) Molero, H.; Bartlett, B. F.; Tysoe, W. T. The hydrogenation of acetylene catalyzed by palladium: hydrogen pressure dependence. *J. Catal.* **1999**, *181*, 49–56.
- (7) Zhao, Y.; Wang, J.; Bao, Z.; Xing, H.; Zhang, Z.; Su, B.; Yang, Q.; Yang, Y.; Ren, Q. Adsorption separation of acetylene and ethylene in a highly thermostable microporous metal-organic framework. *Sep. Purif. Technol.* **2018**, *195*, 238–243.
- (8) Wen, H. M.; Li, B.; Wang, H.; Krishna, R.; Chen, B. High acetylene/ethylene separation in a microporous zinc (II) metal-organic framework with low binding energy. *Chem. Commun.* **2016**, *52*, 1166–1169.
- (9) Cui, X. L.; Chen, K. J.; Xing, H. B.; Yang, Q. W.; Krishna, R.; Bao, Z. B.; Wu, H.; Zhou, W.; Dong, X. L.; Han, Y. Pore chemistry and size control in hybrid porous materials for acetylene capture from ethylene. *Science* **2016**, *353*, 141–144.
- (10) Hu, T. L.; Wang, H. L.; Li, B.; Krishna, R.; Wu, H.; Zhou, W.; Zhao, Y. F.; Han, Y.; Wang, X.; Zhu, W. D.; Yao, Z. Z.; Xiang, S. C.; Chen, B. Microporous metal-organic framework with dual functionalities for highly efficient removal of acetylene from ethylene/acetylene mixtures. *Nat. Commun.* **2015**, *6*, 7328.

- (11) Wang, J.; Xie, D.; Zhang, Z.; Yang, Q.; Xing, H.; Yang, Y.; Ren, Q.; Bao, Z. Efficient adsorption separation of acetylene and ethylene via supported ionic liquid on metal-organic framework. *AIChE J.* **2017**, *63*, 2165–2175.
- (12) Li, L.; Lin, R.-B.; Krishna, R.; Wang, X.; Li, B.; Wu, H.; Li, J.; Zhou, W.; Chen, B. Efficient separation of ethylene from acetylene/ethylene mixtures by a flexible-robust metal-organic framework. *J. Mater. Chem. A* **2017**, *5*, 18984–18988.
- (13) Lin, R.-B.; Li, L.; Wu, H.; Arman, H.; Li, B.; Lin, R.-G.; Zhou, W.; Chen, B. Optimized separation of acetylene from carbon dioxide and ethylene in a microporous material. *J. Am. Chem. Soc.* **2017**, *139*, 8022–8028.
- (14) Metropolis, N.; Rosenbluth, A. W.; Rosenbluth, M. N.; Teller, A. H.; Teller, E. Equation of state calculations by very fast computing machines. *J. Chem. Phys.* **1953**, *21*, 1087–1092.
- (15) Chung, Y.; Na, B. K.; Song, H. K. Short-cut evaluation of pressure swing adsorption systems. *Comput. Chem. Eng.* **1998**, *22*, S637–S640.
- (16) Langmuir, I. The constitution and fundamental properties of solids and liquids. *J. Am. Chem. Soc.* **1916**, *38*, 2221–2295.
- (17) Freundlich, H. M. F. Over the adsorption in solution. *J. Phys. Chem.* **1906**, *57*, 385–471.
- (18) Redlich, O.; Peterson, D. L. A useful adsorption isotherm. *J. Phys. Chem.* **1959**, *63*, 1024–1026.
- (19) Hu, T.-L.; Wang, H.; Krishna, R.; Wu, H.; Zhou, W.; Zhao, Y.; Han, Y.; Wang, X.; Zhu, W.; Yao, Z.; Xiang, S.; Chen, B. Microporous metal-organic framework with dual functionalities for high efficient removal of acetylene from ethylene/acetylene mixtures. *Nat. Commun.* **2015**, *6*, 7328.
- (20) Newalkar, B. L.; Choudary, N. V.; Turaga, U. T.; Vijayalakshmi, R. P.; Kumar, P.; Komarneni, S.; Bhat, T. S. G. Potential adsorbent for light hydrocarbon separation: role of SBA-15 framework porosity. *Chem. Mater.* **2003**, *15*, 1474–1479.
- (21) Pu, S.; Wang, J.; Li, L.; Zhang, Z.; Bao, Z.; Yang, Q.; Yang, Y.; Xing, H.; Ren, Q. Performance comparison of metal-organic framework extrudates and commercial zeolite for ethylene/ethane separation. *Ind. Eng. Chem. Res.* **2018**, *57*, 1645–1654.
- (22) Pellenq, R. J.-M.; Kushima, A.; Shahsavari, R.; Van Vleet, K. J.; Buehler, M. J.; Yip, S.; Ulm, F.-J. A realistic molecular model of cement hydrates. *Proc. Natl. Acad. Sci. U. S. A.* **2009**, *106*, 16102.
- (23) BIOVIA. Dassault Systèmes. *Materials Studio 2020*; BIOVIA: San Diego, CA. 2019.
- (24) Lasich, M. Upgrading wood gas using bentonite clay: a multiscale modelling and simulation study. *ACS Omega* **2020**, *5*, 11068–11074.
- (25) Peng, D. Y.; Robinson, D. B. A new two-constant equation of state. *Ind. Eng. Chem. Fundam.* **1976**, *15*, 59–64.
- (26) Sun, H. COMPASS: an ab initio force-field optimized for condensed-phase applications overview with details on alkane and benzene compounds. *J. Phys. Chem. B* **1998**, *102*, 7338–7364.
- (27) Ewald, P. P. Die Berechnung optischer und elektrostatischer Gitterpotentiale. *Ann. Phys.* **1921**, *369*, 253–287.
- (28) Eaton, J. W.; Bateman, D.; Hauberg, S. *GNU Octave Version 5.1.0 Manual: a High-Level Interactive Language for Numerical Computations*; <https://www.gnu.org/software/octave/doc/v5.1.0/> (accessed Feb 28, 2020).